Thermal Fluctuations and Framework Flexibility of IRMOF-1 upon CH_4 and CO_2 Adsorption

Shivam Parashar†, Nicholas J. Corrente† and Alexander V. Neimark†, *

†Department of Chemical and Biochemical Engineering, Rutgers, The State University of New Jersey, Piscataway, New Jersey 08854, United States

*Email: aneimark@rutgers.edu

ABSTRACT: Flexibility of metal-organic frameworks (MOFs) plays an important role in their applications for adsorption separations, energy and gas storage, and drug delivery. Here, we demonstrate that thermal fluctuations and flexibility of the host framework affect adsorption of guest molecules, which in turn exert a significant adsorption stress, up to 0.1 GPa, on the framework causing its deformation. We find that in contrast with expected gradual swelling during adsorption, framework deformation is non-monotonic with sharp contraction during the pore filling followed by partial expansion. As an important example, we study adsorption of CH_4, and CO_2 on iso-reticular IRMOF-1 crystal at different temperatures using an original computational scheme of iterative grand canonical Monte Carlo (GCMC) and isothermal-isobaric ensemble molecular dynamics (NPT-MD) simulations. The effects or non-monotonic framework flexibility are confirmed by quantitative agreement with adsorption experiments and are expected to be characteristic to different degrees to other MOFs.

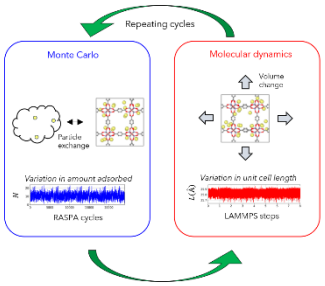

1. Introduction

Metal-organic frameworks (MOFs) are a popular class of nanoporous materials owing to their high surface area, tunability, and stability and are being explored for gas storage, separations, and carbon sequestration. Composed of metal nodes connected by organic linkers, single molecular thin MOF structures experience thermal fluctuations, which cause their intrinsic molecular level flexibility. When guest molecules are introduced into the host framework, they exert a noticeable stress. As a result, the framework may deform changing preferential sites of adsorption and energy landscape within pore compartments. MOF flexibility allows for advanced practical applications such as high-precision separations, detecting traces of organic molecules, slow release of drugs, biosensing, supercapacitors, and energy storage among the others.[1,2-11]

In conventional consideration of adsorption of guest molecules, the host framework is assumed rigid allowing to calculate adsorption isotherms using the conventional grand canonical Monte Carlo (GCMC) simulations.[12] The rigid framework assumption simplifies calculations of adsorption isotherms and is generally accurate. But depending on the framework chemistry, temperature, and nature of the gas molecules, the effects of flexibility must be accounted for. All MOFs deform to different extent upon adsorption of guest molecules. Most prominent examples include significant (up to ~100%) swelling[13], non-monotonic deformation of mesoporous MOFs due to capillary condensation[14], and adsorption-induced framework transformations, like gate opening[15], breathing transitions[16], and negative gas adsorption.[17] Even though the volumetric changes in the framework might be negligible, the thermal fluctuations of the framework atoms can impact adsorption.[18-20] The intrinsic flexibility is relevant when the pore sizes are comparable with the guest molecule size, thereby affecting the transport and accessibility of guest molecules in tight pore spaces. Accounting for intrinsic flexibility when compared to rigid simulation reveals three major conclusions. First, intrinsic flexibility can either reduce or increase the adsorption capacity in comparison to the rigid framework.[21] Second, the pore size distribution becomes wider for flexible framework compared to the rigid ones.[19] Third, accounting for intrinsic framework flexibility is important to accurately predict the adsorption at dilute concentrations.[20,21]

Several attempts have been made to model flexibility upon gas adsorption in MOFs. [20-27] Effects of framework flexibility require combination of GCMC and molecular dynamics (MD) to account for movement of framework atoms. This is achieved by introducing flexible forcefields and using different hybrid MD+GCMC schemes, some of which have been implemented using open source packages LAMMPS,[28] RASPA,[29] Cassandra,[30] NAMD[31] and GOMC.[27, 32] Intrinsic framework flexibility without volumetric deformation of the unit cell is directly modeled by MD simulations in the NVT ensemble alternated with GCMC simulation. [22, 23, 27] Baucom et al.[22] modelled adsorption and diffusion of CO_2 in Cu-BTC framework using hybrid NVT MD simulations with GCMC moves in LAMMPS. The authors concluded that adsorption capacity in flexible simulations is lower compared to rigid simulations and agrees well with the

experiments. Flexible snapshot method introduced by Gee and Sholl[18] accounts for the framework flexibility by first equilibrating the volume of empty framework using NPT MD. This is followed by NVT MD simulations, from which several uncorrelated snapshots (~20) are extracted. Then, GCMC simulations are performed on these snapshots and the resulting isotherms are averaged. The flexible snapshot method considers the intrinsic flexibility of the framework by using various initial framework conformations. A similar approach was employed by Shukla and Johnson.[25] Alternatively, intrinsic flexibility can be modeled entirely in the GCMC simulations, which involve movement of framework atoms.[33-35] However, these methods do not account for the effects of volumetric deformations induced by guest-host interactions.

Volumetric deformation can be considered in the osmotic thermodynamic ensemble, which allows for the volume fluctuations at constant framework composition, external pressure, chemical potential, and temperature.[36, 37] Dubbeldam et al.[21] suggested to introduce NVT MD step as trial moves within the GCMC Markov chain simulation, which is accepted with the Metropolis probability. To account for the volume change, the authors included additional NPT MC trial moves with uniform rescaling of the positions of host framework and guest atoms. This hybrid osmotic Monte Carlo (HOMC) method is implemented in RASPA[29] and actively used.[23, 22] Ghoufi and Maurin[38] suggested an alternative HOMC scheme with NPT MD trial moves that alter the framework conformation and volume. The authors applied this method to simulate breathing transitions in MIL-53(Cr) during CO_2 adsorption. Gee et al.[39] used an analogous HOMC scheme for studies of adsorption and diffusion of alcohols in ZIF-8 and ZIF-90. Rogge et al.[40] suggested several modifications of the HOMC approach. Zhao et al.[41] implemented an Osmotic Molecular Dynamics (OMD) scheme based on the implementation of trial MC move for the insertion/deletion of one guest molecule during the MD trajectory in NPT ensemble. Zhang et al.[42] applied an iterative hybrid MC/MD scheme with alternating Gibbs ensemble MC (GEMC) simulations to determine adsorbed amount at given volume and NPT-MD simulations to vary the volume at given adsorption until the adsorption and mechanical equilibrium is attained. The method was demonstrated on modeling structural transition in ZIF-8 during N_2 adsorption.

The most direct method to account for the volumetric deformation during adsorption is a version of hybrid MC/MD, which involves multiple iterations of GCMC and MD in NPT ensemble simulations. The iterative GCMC/NPT-MD method requires an extensive computational time needed for multiple cycles of MD and MC iterations until the convergence to adsorption and mechanical equilibrium is attained. This approach was used in various implementations for modeling adsorption deformation of polymers,[43, 44] zeolites,[23, 45] and other systems,[42, 43, 46-53] but not for MOFs.

In this work, we developed an advanced implementation of the iterative GCMC/NPT-MD method to study the effects of framework flexibility. This approach is demonstrated with examples of CH_4 and CO_2 adsorption on IRMOF-1 at different temperatures. Due to availability of experimental data, IRMOF-1 is an ideal candidate for exploring flexibility effects. IRMOF-1 is a Zn based MOF consisting of ZnO_4 clusters connected together by benzene dicarboxylic acid (BDC) linkers with a simple and small (~25 Å) unit cell. IRMOF-1 is a relatively rigid MOF. due to its high Young's modulus of 19.5 and 9.5 GPa along the stiffest and softest directions, respectively.[16] Interestingly, IRMOF-1 exhibits the negative thermal expansion: it contracts upon increase in temperature by 0.1 Å per 100 K.[34] Adsorption induced deformation of IRMOF-1 was studied earlier. Adsorption of CO_2 was studied using hybrid MC/MD implemented in RASPA,[54, 55] but the differences between rigid and flexible simulations were negligible.[29] In another work, the structure flexibility of IRMOF-1 was attributed to the rotation of the linker.[56] Adsorption of Ar and H_2 was compared between GCMC rigid and flexible simulations at 78 K and 298 K with little difference found.[33] It should be noted that the latter study used a semiflexible forcefield, where the benzene dicarboxylic linkers were assumed to be rigid. Also, the extent of deformation upon gas adsorption and the effect of temperature was not considered.

In this work, using the iterative GCMC/NPT-MD simulations of CH_4 and CO_2 adsorption on IRMOF-1 at three different temperatures, we discover peculiar mechanisms of adsorption deformation on MOFs. We find that the deformation during adsorption in not monotonic: the framework shrinks in the process of pore filling and expands once the pores are filled. The framework contraction leads to a decrease of adsorption capacity and a shift of the pore filling step that quantitatively agrees with experimental measurements.

2. Methods

The crystallographic structure of IRMOF-1 was taken from reference[57]. CH_4 is modelled as a Lennard-Jones (LJ) particle with parameters from reference[58]. These parameters are slightly different from the standard DACNIS parameters. They were modified to predict accurately the adsorption isotherm of rigid IRMOF-1 compared to experiments at 92 K.[58] CH_4 simulations are performed at 92, 102, and 110 K. This range is chosen due to availability of experimental isotherms at these temperatures.[58]

Adsorption induced deformation simulations were performed using the iterative GCMC/NPT-MD method which involves multiple iterations of alternating MD in LAMMPS and MC in RASPA simulation steps. Iterations are continued until the adsorption and mechanical equilibrium is reached. The LAMMPS data file with forcefield parameters was generated using the LAMMPS interface software.[59] The external stress on the framework is assumed to be equal to the external

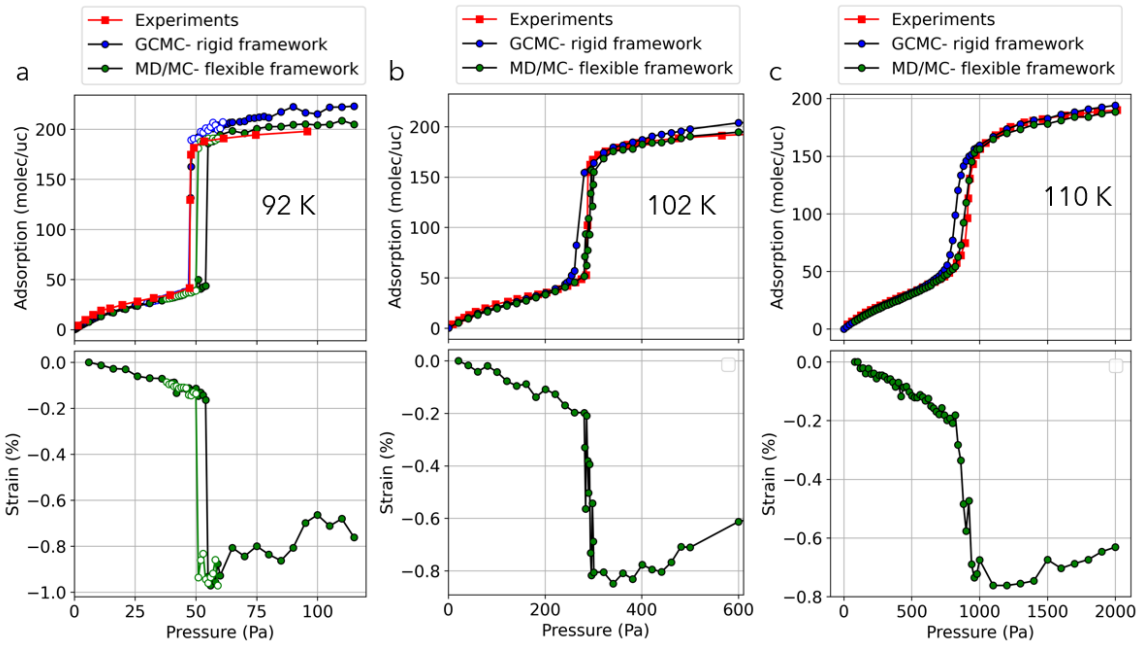

Figure 1: Adsorption and strain isotherms of CH_4 on IRMOF-1 at (a) 92 K, (b) 102 K, and (c) 110 K. Experimental isotherms are taken from reference[58]. Note a narrow hysteresis between adsorption (dark green) and desorption (light green) isotherms at 92K.

reservoir pressure of the gas phase, $\sigma = P_{ext}$. The time step of MD simulations is 1 fs. Each MD iteration is performed for 1 ns which is long enough to achieve mechanical equilibrium. Only isotropic deformations were considered due to the symmetry of IRMOF-1. Nose-hoover thermostat and barostat were employed with time constant of 100 and 1000 timesteps, respectively. PPPM method was used to account for columbic interaction with relative force accuracy of 10^{-6}. The flexibility of IRMOF-1 during MD simulations was modelled using the forcefield as described in reference[34]. In this forcefield, zinc and oxygen atoms are held together by LJ and Coulombic interactions, whereas, the linker atoms are held by bonds, angles, dihedrals, improper, LJ and Coulombic interactions, see Supporting Information Figure S1. The VdW interactions were shifted to zero at a cutoff distance of 12 Å in both MD and MC. Although the LJ parameters between the framework atoms were significantly different in flexible forcefield, the solid-fluid interaction parameters were taken the same as in rigid MC simulations.

During the MC simulations, the framework is kept rigid, and the translation, rotation, reinsertion, and exchange moves are performed on the gas molecules. During each MC iteration, 10,000 RASPA cycles were performed prior to switching to the MD stage. Coulombic interactions between CO_2 and IRMOF-1 were accounted using Ewald summations. We start with MD simulations to relax the structure and take the last snapshot of the framework for performing the GCMC simulations. GCMC and NPT-MD simulations are iterated 12 times, which was shown sufficient for reaching an equilibrated cell length and amount adsorbed. The results are averaged over the last half of the hybrid simulations. A characteristic example is shown in Supporting Information (Figure S2) presenting the fluctuations of the box length, L_z, and the number of particles in the unit cell, N, during alternating MC and MD simulation steps.

3. Results and Discussion

Figure 1 shows the adsorption and strain isotherms calculated using the iterative GCMC/NPT-MD simulations of CH_4 adsorption on IRMOF-1 at 92, 102,

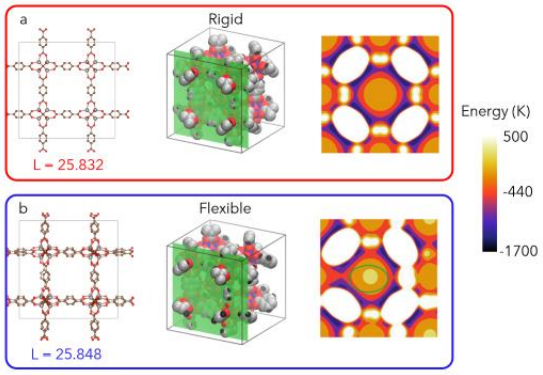

Figure 2: Framework snapshots and solid-fluid energy map for CH_4 adsorption on IRMOF-1 along a selected plane. (a) Rigid structure, (b) Flexible structure.

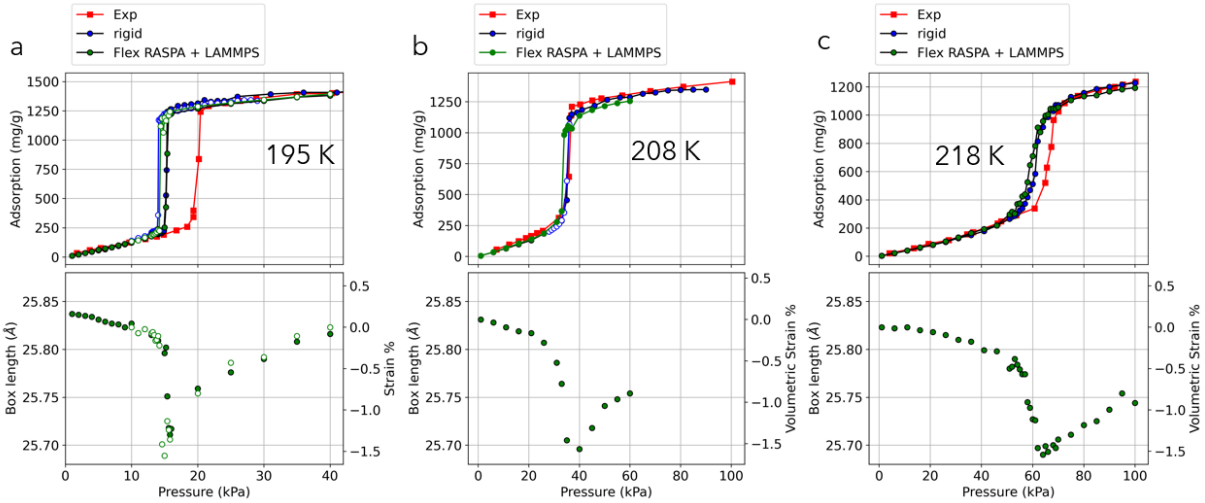

Figure 3: Adsorption and strain isotherms of CO_2 on IRMOF-1 at (a) 195 K, (b) 208 K, and (c) 218 K. Experimental isotherms are taken from reference[60].

and 110 K.[58] We observe elastic contraction prior to the pore filling transition, characteristic stepwise contraction at the transition, and relaxation with minor expansion after the transition. The maximum volumetric strain for CH_4 is ~0.9 % at 92 K, ~0.8 % at 102 K, and ~0.7 % at 110 K. Within the elastic approximation, the adsorption induced volumetric strain, ϵ, is proportional to the difference between the adsorption stress, σ_a, exerted by guest molecules and the external pressure, p,[16,61]

$$\epsilon = -(p - \sigma_a)/K \qquad (1)$$

where K is the volumetric modulus reported for IRMOF-1 in the range 0f 3-15 GPa.[62-64] Assuming K=10 GPa, the adsorption stress causing ~1% contraction of the order of negative 0.1 GPa.

There are three visible differences between the rigid and flexible isotherms. First, the flexible isotherm exhibits reduced adsorption capacity, which matches well with experiments at all temperatures. This is due to the contraction of the framework upon adsorption. Second, the pore filling transition in flexible isotherm is shifted to higher pressure compared to the rigid isotherm. This is due to the reduced attractive potential between the framework atoms and guest molecules. Figure 2 shows the framework atoms snapshots and surface energy map along the chosen plane during the rigid and flexible simulation. Due to thermal fluctuation of framework atoms during the flexible simulations, the surface energy map has patches of lower attractive energy, Figure 2b. The calculation of 1D solid-fluid energy histogram for the ideal and flexible snapshots of IRMOF-1 revealed that the flexible frameworks have 1.8 % lower attractive energy compared to the ideal symmetric framework (supporting information Figure S3), resulting in the shift of the pore filling step to higher pressure. This shift was also observed during the canonical ensemble Monte Carlo simulations.[65]

Third, at 92 K, the flexible simulations exhibit a minor hysteresis whereas the rigid simulation does not. This is because prior to condensation the unit cell length is 25.900 Å, slightly higher than the rigid structure 25.832 Å, results in reduced solid-fluid attractions and hence a delayed condensation step. During desorption however, the contracted box length of 25.800 Å (slightly smaller than the rigid structure 25.832 Å) results in transition at lower pressure. Therefore, the difference in the unit cell size before the adsorption and desorption transitions results in a minor hysteresis at 92 K. As the temperature increases, both the simulated and experimental isotherms become continuous and reversible.

Overall, the experimental isotherms match more closely with the flexible simulated isotherms at 102 and 110 K, and with the rigid simulated isotherm at 92 K. This could be attributed to the CH_4 interaction parameters taken from ref. [58], which were adjusted to fit the experimental isotherm at 92 K in MC simulations with a rigid framework.

Figure 3 compares the rigid, flexible, and experimental isotherms of CO_2 at 195, 208, and 218 K. For CO_2, the maximum volumetric contraction is larger (1.5%) compared to CH_4 (1%). Despite the larger deformation, the adsorption capacity in flexible simulations is only marginally smaller compared to rigid, and the pore filling steps in flexible and rigid simulations are almost identical. Overall, the differences between rigid and flexible simulations of CO_2 are significantly smaller compared to differences observed for CH_4 isotherms. This can be attributed to the strength of the fluid-fluid interactions: CO_2-CO_2 interaction is stronger than CH_4-CH_4. The weaker CH_4-CH_4 interactions imply that even a

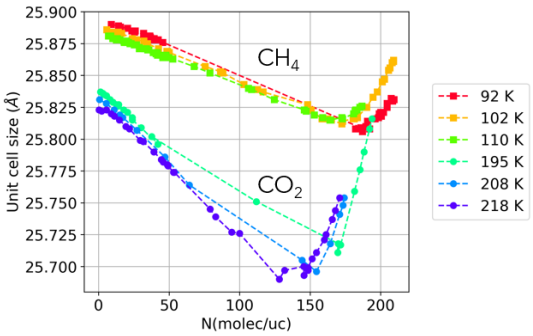

Figure 4: Dependence of IRMOF-1 unit cell length upon adsorption of CH_4 at 92, 102, and 110 K and CO_2 at 195, 208, and 218 K.

slight alteration in the solid potential can markedly affect the pore filling step and adsorption capacity. Conversely, for CO_2, the primary source of attraction stems from fluid-fluid interactions, which overshadow the solid-

fluid interactions. Consequently, despite a 1.8% reduction in solid-fluid interactions in the flexible snapshots, the isotherms exhibit minimal variation. (Supporting Information, Figure S3)

The experimental isotherm in Figure 3 shown in red, matches exactly at 208 K. At temperatures of 195 and 218 K, both the simulations and experiments correspond well in terms of adsorption capacity and adsorption before the pore filling step. But simulations predict the pore filling steps to be at lower pressure compared to the experimental observations.

Figure 4 illustrates the dependence of the unit cell size against the CO_2 and CH_4 adsorption at various temperatures. Note that the initial unit cell size decreases as temperature increases due to the negative thermal expansion coefficient of IRMOF-1. [34] This explains the difference in the unit cell lengths on an empty framework. Upon gas adsorption but before the complete pore filling, the unit cell size decreases linearly with the number of adsorbed gas molecules. Notably, the slope of the plot is steeper for CO_2 due to its stronger interactions with IRMOF-1 compared to CH_4. This effect of the reduction of the unit cell length and hence the pore size is characteristic to all microporous materials, since the adsorbed molecules play roles of molecular springs attracting opposite framework atoms.[16, 61] Adsorbed molecules exert a negative adsorption stress causing the framework contraction. The maximum contraction corresponds to the pore filling with loosely packed guest molecules. Further increase of pressure caused re-packing and densification of the adsorbed phase to accommodate addition molecules, which exert repulsive positive stress on the framework facilitating its expansion.

4. Conclusions

We demonstrate that IRMOF-1, which is often considered a rigid MOF, exhibits volumetric contraction of up to ~1% upon CH_4 adsorption and ~1.5% upon CO_2 adsorption. In the case of CH_4, this contraction reduces to 0.9 and 0.8 % with increase in temperature to 102 and 110 K, respectively. Framework contraction causes a decrease of the adsorption capacity and a shift the adsorption isotherm to lower pressure, resulting in a better match to experiments at 102 and 110 K. In the case of CO_2, the maximum contraction is slightly higher, around 1.5%, due to the stronger interactions of CO_2 compared to CH_4 which stems from additional coulombic contribution. However, the differences in the adsorption capacity and pore filling steps in rigid and flexible simulations for CO_2 are negligible compared to CH_4.

The cause of framework contraction upon the pore filling is attributed to the attractive fluid-solid interactions with adsorbed molecules acting as molecular springs pulling framework atoms inwards within the pores. The adsorption stress exerted by the guest molecules causing the framework contraction is estimated of up to 0.1 GPa. The contraction stage is followed by the framework expansion upon pore filling due to packing effects and restructuring to accommodate additional molecules. Such non-monotonic deformation is characteristic, to different extent, to all microporous materials.

On the methodological side, we have implemented the iterative GCMC/NPT-MD scheme using LAMMPS and RASPA packages and demonstrated the efficiency of this approach. It is worth noting that IRMOF-1 is a relatively simple system, and the computational challenge increases for frameworks with larger unit cells.

The influence of temperature on the MOF unit cell size and conformation is frequently overlooked during adsorption simulations, with the assumption that the framework volume remains constant across all temperatures. The presented example shows that the thermal fluctuations of the framework are important and cannot be ignored even when the deformation effects are minor. The crystallographic structures published in the databases must be MD equilibrated at given temperature prior to generating the adsorption isotherm in the MC simulations.

ASSOCIATED CONTENT

Supporting Information

1. Details of the iterative GCMC/NPT-MD simulations in RASPA and LAMMPS separately.
2. Comparison of RASPA and LAMMPS, and RASPA + LAMMPS simulations.
3. Adsorption isotherms on rigid frameworks of different box lengths.

AUTHOR INFORMATION

Corresponding Author

Alexander V. Neimark – Department of Chemical and Biochemical Engineering, Rutgers, The State University of New Jersey, Piscataway, New Jersey 08854, United States; orcid.org/0000-0002-3443-0389; Email: aneimark@rutgers.edu

Author

Shivam Parashar – Department of Chemical and Biochemical Engineering, Rutgers, The State University of New Jersey, Piscataway, New Jersey 08854, United States; orcid.org/ 0000-0002-0323-7391.

Author

Nicholas J. Corrente – Department of Chemical and Biochemical Engineering, Rutgers, The State University of New Jersey, Piscataway, New Jersey 08854, United States.

Author Contributions

All authors have given approval to the final version of the manuscript.

Notes

The authors declare no competing financial interest.

ACKNOWLEDGMENT

This work is supported by the National Science Foundation (CBET Grant 18334339).

REFERENCES

1. Senkovska, I.; Bon, V.; Abylgazina, L.; Mendt, M.; Berger, J.; Kieslich, G.; Petkov, P.; Luiz Fiorio, J.; Joswig, J. O.; Heine, T.; Schaper, L.; Bachetzky, C.; Schmid, R.; Fischer, R. A.; Pöppl, A.; Brunner, E.; Kaskel, S., Understanding MOF Flexibility: An Analysis Focused on Pillared Layer MOFs as a Model System. *Angewandte Chemie International Edition* **2023,** *62* (33).

2. Binaeian, E.; Nabipour, H.; Ahmadi, S.; Rohani, S., The green synthesis and applications of biological metal-organic frameworks for targeted drug delivery and tumor treatments. *Journal of Materials Chemistry B* **2023,** *11* (48), 11426-11459.

3. Du, J. R.; Shi, F. Y.; Wang, K.; Han, Q.; Shi, Y. J.; Zhang, W.; Gao, Y. N.; Dong, B.; Wang, L.; Xu, L., Metal-organic framework-based biosensing platforms for diagnosis of bacteria-induced infectious diseases. *Trac-Trends in Analytical Chemistry* **2024,** *175*.

4. Khosroshahi, N.; Bakhtian, M.; Asadi, A.; Safarifard, V., Revolutionizing energy storage: the emergence of MOF/MXene composites as promising supercapacitors. *Nano Express* **2023,** *4* (4).

5. Ramu, S.; Kainthla, I.; Chandrappa, L.; Shivanna, J. M.; Kumaran, B.; Balakrishna, R. G., Recent advances in metal organic frameworks-based magnetic nanomaterials for waste water treatment. *Environmental Science and Pollution Research* **2024,** *31* (1), 1589-1606.

6. Shalini, S.; Naveen, T. B.; Durgalakshmi, D.; Balakumar, S.; Rakkesh, R. A., Progress in flexible supercapacitors for wearable electronics using graphene-based organic frameworks. *Journal of Energy Storage* **2024,** *86*.

7. Smoljan, C. S.; Snurr, R. Q.; Farha, O. K., 3-dimensional linker-based metal-organic frameworks for sub-angstrom control and enhanced thermal stability. *Journal of Materials Research* **2024,** *39* (7), 1047-1056.

8. Su, H. H.; Lv, S. H.; Song, H. J.; Shi, K. L.; Zhu, J. Y.; Zhang, Y. T., Recent advances in continuous zirconium-based metal-organic framework membranes for high-precision separation. *Separation and Purification Technology* **2024,** *345*.

9. Wang, D. D.; Wu, Q.; Ren, X. L.; Niu, M.; Ren, J.; Meng, X. W., Tunable Zeolitic Imidazolate Framework-8 Nanoparticles for Biomedical Applications. *Small Methods* **2024,** *8* (3).

10. Yusuf, M.; Kumar, R.; Khan, M. A.; Ahmed, M. J.; Otero, M.; Prabhu, S. M.; Son, M.; Hwang, J. H.; Lee, W. H.; Jeon, B. H., Metal-organic framework-based composites for biogas and natural gas uptake: An overview of adsorption and storage mechanisms of gaseous fuels. *Chemical Engineering Journal* **2023,** *478*.

11. Zhu, X. G.; Xu, J. Q.; Ling, G. X.; Zhang, P., Tunable metal-organic frameworks assist in catalyzing DNAzymes with amplification platforms for biomedical applications. *Chemical Society Reviews* **2023,** *52* (21), 7549-7578.

12. Formalik, F.; Shi, K.; Joodaki, F.; Wang, X.; Snurr, R. Q., Exploring the Structural, Dynamic, and Functional Properties of Metal-Organic Frameworks through Molecular Modeling. *Advanced Functional Materials* **2023**.

13. Mellot-Draznieks, C.; Serre, C.; Surblé, S.; Audebrand, N.; Férey, G., Very Large Swelling in Hybrid Frameworks: A Combined Computational and Powder Diffraction Study. *Journal of the American Chemical Society* **2005,** *127* (46), 16273-16278.

14. Sung Cho, H.; Deng, H.; Miyasaka, K.; Dong, Z.; Cho, M.; Neimark, A. V.; Ku Kang, J.; Yaghi, O. M.; Terasaki, O., Extra adsorption and adsorbate superlattice formation in metal-organic frameworks. *Nature* **2015,** *527* (7579), 503-507.

15. Fairen-Jimenez, D.; Moggach, S. A.; Wharmby, M. T.; Wright, P. A.; Parsons, S.; Düren, T., Opening the Gate: Framework Flexibility in ZIF-8 Explored by Experiments and Simulations. *Journal of the American Chemical Society* **2011,** *133* (23), 8900-8902.

16. Coudert, F.-X.; Boutin, A.; Fuchs, A. H.; Neimark, A. V., Adsorption Deformation and Structural Transitions in Metal–Organic Frameworks: From the Unit Cell to the Crystal. *The Journal of Physical Chemistry Letters* **2013,** *4* (19), 3198-3205.

17. Krause, S.; Evans, J. D.; Bon, V.; Senkovska, I.; Iacomi, P.; Kolbe, F.; Ehrling, S.; Troschke, E.; Getzschmann, J.; Többens, D. M.; Franz, A.; Wallacher, D.; Yot, P. G.; Maurin, G.; Brunner, E.; Llewellyn, P. L.; Coudert, F.-X.; Kaskel, S., Towards general network architecture design criteria for negative gas adsorption transitions in ultraporous frameworks. *Nature Communications* **2019,** *10* (1).

18. Gee, J. A.; Sholl, D. S., Effect of Framework Flexibility on C8 Aromatic Adsorption at High Loadings in Metal–Organic Frameworks. *The Journal of Physical Chemistry C* **2015,** *120* (1), 370-376.

19. Witman, M.; Ling, S.; Jawahery, S.; Boyd, P. G.; Haranczyk, M.; Slater, B.; Smit, B., The Influence of Intrinsic Framework Flexibility on Adsorption in Nanoporous Materials. *Journal of the American Chemical Society* **2017,** *139* (15), 5547-5557.

20. Yu, Z.; Anstine, D. M.; Boulfelfel, S. E.; Gu, C.; Colina, C. M.; Sholl, D. S., Incorporating Flexibility Effects into Metal–Organic Framework Adsorption Simulations Using Different Models. *ACS Applied Materials & Interfaces* **2021,** *13* (51), 61305-61315.

21. Agrawal, M.; Sholl, D. S., Effects of Intrinsic Flexibility on Adsorption Properties of Metal–Organic Frameworks at Dilute and Nondilute Loadings. *ACS Applied Materials & Interfaces* **2019,** *11* (34), 31060-31068.

22. Baucom, T.; Budhathoki, S.; Steckel, J. A., Effect of Flexibility in Molecular Simulations of Carbon Dioxide Adsorption and Diffusion in a Cuprous Triazolate Framework.

The Journal of Physical Chemistry C **2023,** *127* (35), 17524-17531.

23. Caro-Ortiz, S.; Zuidema, E.; Dekker, D.; Rigutto, M.; Dubbeldam, D.; Vlugt, T. J. H., Adsorption of Aromatics in MFI-Type Zeolites: Experiments and Framework Flexibility in Monte Carlo Simulations. *The Journal of Physical Chemistry C* **2020,** *124* (39), 21782-21797.

24. Daou, A. S. S.; Findley, J. M.; Fang, H.; Boulfelfel, S. E.; Ravikovitch, P. I.; Sholl, D. S., Quantifying Impact of Intrinsic Flexibility on Molecular Adsorption in Zeolites. *The Journal of Physical Chemistry C* **2021,** *125* (9), 5296-5305.

25. Shukla, P. B.; Johnson, J. K., Impact of Loading-Dependent Intrinsic Framework Flexibility on Adsorption in UiO-66. *The Journal of Physical Chemistry C* **2022,** *126* (41), 17699-17711.

26. Witman, M.; Wright, B.; Smit, B., Simulating Enhanced Methane Deliverable Capacity of Guest Responsive Pores in Intrinsically Flexible MOFs. *The Journal of Physical Chemistry Letters* **2019,** *10* (19), 5929-5934.

27. Barhaghi, M. S.; Crawford, B.; Schwing, G.; Hardy, D. J.; Stone, J. E.; Schwiebert, L.; Potoff, J.; Tajkhorshid, E., py-MCMD: Python Software for Performing Hybrid Monte Carlo/Molecular Dynamics Simulations with GOMC and NAMD. *Journal of Chemical Theory and Computation* **2022,** *18* (8), 4983-4994.

28. Thompson, A. P.; Aktulga, H. M.; Berger, R.; Bolintineanu, D. S.; Brown, W. M.; Crozier, P. S.; in 't Veld, P. J.; Kohlmeyer, A.; Moore, S. G.; Nguyen, T. D.; Shan, R.; Stevens, M. J.; Tranchida, J.; Trott, C.; Plimpton, S. J., LAMMPS - a flexible simulation tool for particle-based materials modeling at the atomic, meso, and continuum scales. *Computer Physics Communications* **2022,** *271*.

29. Dubbeldam, D.; Calero, S.; Ellis, D. E.; Snurr, R. Q., RASPA: molecular simulation software for adsorption and diffusion in flexible nanoporous materials. *Molecular Simulation* **2015,** *42* (2), 81-101.

30. Shah, J. K.; Marin-Rimoldi, E.; Mullen, R. G.; Keene, B. P.; Khan, S.; Paluch, A. S.; Rai, N.; Romanielo, L. L.; Rosch, T. W.; Yoo, B.; Maginn, E. J., Cassandra: An open source Monte Carlo package for molecular simulation. *Journal of Computational Chemistry* **2017,** *38* (19), 1727-1739.

31. Phillips, J. C.; Hardy, D. J.; Maia, J. D. C.; Stone, J. E.; Ribeiro, J. V.; Bernardi, R. C.; Buch, R.; Fiorin, G.; Hénin, J.; Jiang, W.; McGreevy, R.; Melo, M. C. R.; Radak, B. K.; Skeel, R. D.; Singharoy, A.; Wang, Y.; Roux, B.; Aksimentiev, A.; Luthey-Schulten, Z.; Kalé, L. V.; Schulten, K.; Chipot, C.; Tajkhorshid, E., Scalable molecular dynamics on CPU and GPU architectures with NAMD. *The Journal of Chemical Physics* **2020,** *153* (4).

32. Nejahi, Y.; Barhaghi, M. S.; Schwing, G.; Schwiebert, L.; Potoff, J., Update 2.70 to "GOMC: GPU Optimized Monte Carlo for the simulation of phase equilibria and physical properties of complex fluids". *SoftwareX* **2021,** *13*.

33. Greathouse, J. A.; Kinnibrugh, T. L.; Allendorf, M. D., Adsorption and Separation of Noble Gases by IRMOF-1: Grand Canonical Monte Carlo Simulations. *Industrial & Engineering Chemistry Research* **2009,** *48* (7), 3425-3431.

34. Dubbeldam, D.; Walton, K. S.; Ellis, D. E.; Snurr, R. Q., Exceptional Negative Thermal Expansion in Isoreticular Metal–Organic Frameworks. *Angewandte Chemie International Edition* **2007,** *46* (24), 4496-4499.

35. Vlugt, T. J. H.; Schenk, M., Influence of Framework Flexibility on the Adsorption Properties of Hydrocarbons in the Zeolite Silicalite. *The Journal of Physical Chemistry B* **2002,** *106* (49), 12757-12763.

36. Bousquet, D.; Coudert, F.-X.; Fossati, A. G. J.; Neimark, A. V.; Fuchs, A. H.; Boutin, A., Adsorption induced transitions in soft porous crystals: An osmotic potential approach to multistability and intermediate structures. *The Journal of Chemical Physics* **2013,** *138* (17).

37. Coudert, F.-X.; Jeffroy, M.; Fuchs, A. H.; Boutin, A.; Mellot-Draznieks, C., Thermodynamics of Guest-Induced Structural Transitions in Hybrid Organic–Inorganic Frameworks. *Journal of the American Chemical Society* **2008,** *130* (43), 14294-14302.

38. Ghoufi, A.; Maurin, G., Hybrid Monte Carlo Simulations Combined with a Phase Mixture Model to Predict the Structural Transitions of a Porous Metal–Organic Framework Material upon Adsorption of Guest Molecules. *The Journal of Physical Chemistry C* **2010,** *114* (14), 6496-6502.

39. Gee, J. A.; Chung, J.; Nair, S.; Sholl, D. S., Adsorption and Diffusion of Small Alcohols in Zeolitic Imidazolate Frameworks ZIF-8 and ZIF-90. *The Journal of Physical Chemistry C* **2013,** *117* (6), 3169-3176.

40. Rogge, S. M. J.; Goeminne, R.; Demuynck, R.; Gutiérrez-Sevillano, J. J.; Vandenbrande, S.; Vanduyfhuys, L.; Waroquier, M.; Verstraelen, T.; Van Speybroeck, V., Modeling Gas Adsorption in Flexible Metal–Organic Frameworks via Hybrid Monte Carlo/Molecular Dynamics Schemes. *Advanced Theory and Simulations* **2019,** *2* (4).

41. Zhao, H.; Pelgrin-Morvan, C.; Maurin, G.; Ghoufi, A., Cutting-edge molecular modelling to unveil new microscopic insights into the guest-controlled flexibility of metal–organic frameworks. *Chemical Science* **2022,** *13* (48), 14336-14345.

42. Zhang, L.; Hu, Z.; Jiang, J., Sorption-Induced Structural Transition of Zeolitic Imidazolate Framework-8: A Hybrid Molecular Simulation Study. *Journal of the American Chemical Society* **2013,** *135* (9), 3722-3728.

43. Morgan, W. J.; Anstine, D. M.; Colina, C. M., Temperature Effects in Flexible Adsorption Processes for Amorphous Microporous Polymers. *The Journal of Physical Chemistry B* **2022,** *126* (33), 6354-6365.

44. Hua, L.; Zhang, C.; Shomali, A.; Coasne, B.; Derome, D.; Carmeliet, J., Sorption-Deformation Interplay in Hierarchical Porous Polymeric Structures Composed of a Slit Pore in an Amorphous Matrix. *Langmuir* **2023,** *39* (32), 11345-11356.

45. Emelianova, A.; Balzer, C.; Reichenauer, G.; Gor, G. Y., Adsorption-Induced Deformation of Zeolites 4A and 13X: Experimental and Molecular Simulation Study. *Langmuir* **2023,** *39* (32), 11388-11397.

46. Jawahery, S.; Simon, C. M.; Braun, E.; Witman, M.; Tiana, D.; Vlaisavljevich, B.; Smit, B., Adsorbate-induced lattice deformation in IRMOF-74 series. *Nature Communications* **2017,** *8* (1).

47. Zhang, J.; Clennell, M. B.; Dewhurst, D. N.; Liu, K., Combined Monte Carlo and molecular dynamics simulation of methane adsorption on dry and moist coal. *Fuel* **2014,** *122*, 186-197.

48. Zhang, J.; Liu, K.; Clennell, M. B.; Dewhurst, D. N.; Pervukhina, M., Molecular simulation of CO2–CH4 competitive adsorption and induced coal swelling. *Fuel* **2015,** *160*, 309-317.

49. Chen, M.; Coasne, B.; Guyer, R.; Derome, D.; Carmeliet, J., Molecular Simulation of Sorption-Induced Deformation in Atomistic Nanoporous Materials. *Langmuir* **2019,** *35* (24), 7751-7758.

50. Wu, J.; Huang, P.; Maggi, F.; Shen, L., Molecular investigation on CO_2-CH_4 displacement and kerogen deformation in enhanced shale gas recovery. *Fuel* **2022,** *315*.

51. Dutta, R. C.; Bhatia, S. K., Transport Diffusion of Light Gases in Polyethylene Using Atomistic Simulations. *Langmuir* **2017,** *33* (4), 936-946.

52. Palmer, J. C.; Debenedetti, P. G., Computer Simulation of Water Sorption on Flexible Protein Crystals. *The Journal of Physical Chemistry Letters* **2012,** *3* (18), 2713-2718.

53. Yang, Y.; Narayanan Nair, A. K.; Sun, S., Sorption and Diffusion of Methane and Carbon Dioxide in Amorphous Poly(alkyl acrylates): A Molecular Simulation Study. *The Journal of Physical Chemistry B* **2020,** *124* (7), 1301-1310.

54. Duane, S.; Kennedy, A. D.; Pendleton, B. J.; Roweth, D., Hybrid Monte Carlo. *Physics Letters B* **1987,** *195* (2), 216-222.

55. Chempath, S.; Clark, L. A.; Snurr, R. Q., Two general methods for grand canonical ensemble simulation of molecules with internal flexibility. *The Journal of Chemical Physics* **2003,** *118* (16), 7635-7643.

56. Dubbeldam, D.; Krishna, R.; Snurr, R. Q., Method for Analyzing Structural Changes of Flexible Metal–Organic Frameworks Induced by Adsorbates. *The Journal of Physical Chemistry C* **2009,** *113* (44), 19317-19327.

57. Eddaoudi, M.; Kim, J.; Rosi, N.; Vodak, D.; Wachter, J.; O'Keeffe, M.; Yaghi, O. M., Systematic Design of Pore Size and Functionality in Isoreticular MOFs and Their Application in Methane Storage. *Science* **2002,** *295* (5554), 469-472.

58. Mazur, B.; Formalik, F.; Roztocki, K.; Bon, V.; Kaskel, S.; Neimark, A. V.; Firlej, L.; Kuchta, B., Quasicontinuous Cooperative Adsorption Mechanism in Crystalline Nanoporous Materials. *The Journal of Physical Chemistry Letters* **2022,** *13* (30), 6961-6965.

59. Boyd, P. G.; Moosavi, S. M.; Witman, M.; Smit, B., Force-Field Prediction of Materials Properties in Metal-Organic Frameworks. *J. Phys. Chem. Lett.* **2017,** *8* (2), 357-363.

60. Millward, A. R., *Adsorption of environmentally significant gases (hydrogen, carbon dioxide, hydrogen sulfide, methane) in metal-organic frameworks*. University of Michigan: 2006.

61. Ravikovitch, P. I.; Neimark, A. V., Density Functional Theory Model of Adsorption Deformation. *Langmuir* **2006,** *22* (26), 10864-10868.

62. Bahr, D. F.; Reid, J. A.; Mook, W. M.; Bauer, C. A.; Stumpf, R.; Skulan, A. J.; Moody, N. R.; Simmons, B. A.; Shindel, M. M.; Allendorf, M. D., Erratum: Mechanical properties of cubic zinc carboxylate IRMOF-1 metal-organic framework crystals [Phys. Rev. B76, 184106 (2007)]. *Physical Review B* **2008,** *77* (5).

63. Mattesini, M.; Soler, J. M.; Ynduráin, F., Ab initiostudy of metal-organic framework-5Zn4O(1,4–benzenedicarboxylate)3: An assessment of mechanical and spectroscopic properties. *Physical Review B* **2006,** *73* (9).

64. Redfern, L. R.; Farha, O. K., Mechanical properties of metal–organic frameworks. *Chemical Science* **2019,** *10* (46), 10666-10679.

65. Li, Z.; Turner, J.; Snurr, R. Q., Computational investigation of hysteresis and phase equilibria of n-alkanes in a metal-organic framework with both micropores and mesopores. *Commun. Chem.* **2023,** *6* (1).